

INVESTIGATION OF THE EFFECTS OF FLUID FLOW ON SRB BIOFILM

Jie Wen, Tingyue Gu and Srdjan Nescic
Institute for Corrosion and Multiphase Technology
Ohio University
342 West State Street
Athens, Ohio 45701

ABSTRACT

Various studies have indicated that sessile bacteria in biofilms, not planktonic bacteria suspended in liquids, are directly responsible for pitting attack on metal surfaces in Microbiologically Influenced Corrosion (MIC). MIC has been detected not only in static fluid systems, but also in flow systems. Fluid flow directly impacts mass transfer and biofilm formation. A sufficiently high linear flow velocity can prevent biofilm establishment or even dislodge an established biofilm. It is difficult to perform experiments using a large flow loop to achieve high linear velocities. Instead, an electrochemical glass cell bioreactor with a cylindrical coupon on a rotating shaft can be used to simulate pipe flow with high linear velocities in MIC research. Mass transfer and wall shear stress similarities can be used to relate the coupon rotational speed in a glass cell and the average linear velocity in the corresponding pipe flow. In this work, ATCC 7757 strain of *Desulfovibrio desulfuricans*, a common strain of sulfate-reducing bacteria (SRB), was used in glass cell experiments to study biofilm behavior under flow conditions. The results confirmed that a high linear flow velocity could indeed prevent SRB biofilm formation.

Keywords: Sulfate reducing bacteria, microbiologically influenced corrosion, biofilm, mass transfer, *Desulfovibrio desulfuricans*

INTRODUCTION

MIC is a major challenge to the oil and gas industry and the problem is growing due to aging equipment and practices such as water flooding used to extract oil from depleting reservoirs. A group of bacteria known as sulfate reducing bacteria (SRB) are often found to be responsible for MIC¹. Acid producing bacteria may also be directly involved in MIC. Some other bacteria may be indirectly involved, such as aerobic biofilm-forming bacteria that provide an anaerobic microenvironment for SRB to thrive.

Water injection or flooding is a common oilfield practice used to increase well pressure in aging wells. Injection water typically comes from nearby aquifer or more often the sea. Seawater contains nutrients sufficient for some bacteria to grow. Untreated seawater carries harmful bacteria such as SRB. Even treated seawater can be a source of SRB inoculum². It was initially believed by some people that MIC normally occurred under stagnant conditions. However, experimental and field results showed that MIC also occurred under flow conditions. At linear velocities of about 0.35 m/s, MIC on AISI 1018 mild steel was reported³. Hydrodynamics and nutrient availability are two key factors influencing biofilm growth in MIC investigations. Fluid flow can enhance mass transfer but it may also produce a high shear that inhibits cell attachment and causes even detachment of an established biofilm⁴. Stoodly et al.⁵ observed that the *Pseudomonas aeruginosa* biofilm pre-grown in a glass flow cell was detached at 3.5 m/s. It was reported that the structure and material properties of SRB biofilms were influenced by the fluid shear⁶. Laboratory research at Ohio University indicated that the fluid flow rate had a considerable impact on MIC corrosion rates of carbon steels⁷. This work presents additional information on the SRB biofilm growth under flow conditions.

METHOD AND THEORY

A rotating cylinder electrode glass cell is a popular device in the study of chemical corrosion under flow conditions. The rotational speed of the cylindrical coupon on a shaft can go as high as 10,000 rpm, which translates into several meters per second in pipe flow linear velocity. From wall shear stress similarity and/or mass transfer coefficient similarity, the coupon rotational speed can be correlated with the linear velocity in pipe flow⁸⁻¹¹.

In fluid mechanics, for flow in the horizontal section of a pipe, the wall shear stress (τ_{pipe}) can be calculated using the pressure drop per unit pipe length (Δp_l) and pipe inner diameter (d_{pipe}) based on the equation below^{12,13},

$$\tau_{pipe} = \frac{\Delta p_l d_{pipe}}{4} \quad (1)$$

In Eq. (1), Δp_l can be calculated based on the definition of friction factor f in horizontal pipe flow as shown below where ρ is the liquid density and u_{pipe} is the average linear velocity.

$$\Delta p_l = \frac{f}{d_{pipe}} \frac{\rho u_{pipe}^2}{2} \quad (2)$$

Combining the two equations above, the following equation is obtained^{13, 14}.

$$\tau_{pipe} = \frac{f}{8} \rho u_{pipe}^2 \quad (3)$$

The friction factor f in Equation (3) can be obtained from the well-known Moody chart¹⁵ given the Reynolds number (Re) and the relative pipe roughness ε/d_{pipe} , or from the implicit Colebrook formula¹³. As an alternative to the Colebrook formula, the explicit formula¹³ below can be used more conveniently to calculate f in turbulent flow,

$$f = \frac{0.25}{\left[\log \left(\frac{\varepsilon}{3.7d_{pipe}} + \frac{5.74}{Re^{0.9}} \right) \right]^2} \quad (4)$$

Eq. (4) is valid for $5 \times 10^3 \leq Re \leq 10^8$ and $10^{-6} \leq \varepsilon/d_{pipe} \leq 10^{-2}$.

By assuming a hydraulically smooth coupon surface, Silverman⁸ derived an empirical correlation for the shear stress on the surface of a rotating cylinder coupon in a glass cell as follows,

$$\tau_{cyl} = 0.079Re^{-0.30}\rho(u_{cyl})^2 = 0.079Re^{-0.30}\rho(0.5\omega d_{cyl})^2 \quad (5a)$$

where Re is the Reynolds number based on the cylinder diameter (d_{cyl}), u_{cyl} the linear velocity on the coupon surface in $\text{cm}\cdot\text{s}^{-1}$, ω angular velocity in radians/s. The units for τ_{cyl} , ρ and d_{cyl} in Equation (5) above are $\text{g}\cdot\text{cm}^{-1}\cdot\text{s}^{-2}$, $\text{g}\cdot\text{cm}^{-3}$ and cm , respectively. By equating τ_{cyl} to τ_{pipe} , Equations (3) to (5) relate the coupon rotational speed in a glass cell to the average linear velocity in pipe flow for achieving the same shear stress on a metal surface.

In MIC studies, the coupon surface may be covered with a biofilm, and it may not be treated as a smooth surface. Equation (5a) can be rewritten below to consider surface roughness (ε) based on an empirical correlation obtained by Sedahmed et al.¹⁶

$$\tau_{cyl} = 0.714Re^{-0.39}(\varepsilon/d_{cyl})^{0.2}\rho(u_{cyl})^2 = 0.714Re^{-0.39}(\varepsilon/d_{cyl})^{0.2}\rho(0.5\omega d_{cyl})^2 \quad (5b)$$

The mass transfer coefficient in fully developed pipe flow can be expressed for large Sc numbers (from 693 to 37,200) as a function of wall shear stress according to Shaw and Hanratty¹⁷,

$$k_{pipe} = 0.0889 \sqrt{\frac{\tau_{pipe}}{\rho}} Sc^{-0.704} \quad (6)$$

where mass transfer coefficient k_{pipe} is in $\text{m}\cdot\text{s}^{-1}$, τ_{pipe} in $\text{kg}\cdot\text{m}^{-1}\cdot\text{s}^{-2}$ and ρ in $\text{kg}\cdot\text{m}^{-3}$. $\sqrt{\tau_{pipe}/\rho}$ is the so-called friction velocity that has the same units as linear velocity and mass transfer coefficient. Equation (6) also applies to annular flow. Sc is the dimensionless Schmidt number defined as $\mu/(\rho D)$ in which D is the diffusion coefficient. The mass transfer coefficient for a rotating cylinder in a glass cell can be expressed as follows⁹,

$$k_{cyl} = \frac{\tau_{cyl}}{\rho u_{cyl}} Sc^{-0.644} \quad (7)$$

which is valid for $200 < Re < 1.5 \times 10^5$ and $3 < Sc < 30,000$. The linear rotation velocity of the cylindrical coupon can be translated into the average linear velocity in pipe flow for different pipe diameters (d_{pipe})

based on the Silverman correlation^{9, 11} for mass transfer coefficient similarity in pipe and annular flows, which states,

$$u_{cyl} = 0.1185 \left[\left(\frac{\mu}{\rho} \right)^{-0.25} \left(\frac{d_{cyl}^{3/7}}{d_{pipe}^{5/28}} \right) Sc^{-0.0857} \right] u_{pipe}^{5/4} \quad (8)$$

where μ is in poise, ρ in $\text{kg}\cdot\text{m}^{-3}$, d_{cyl} and d_{pipe} in m, u_{cyl} and u_{pipe} in $\text{m}\cdot\text{s}^{-1}$.

When u_{cyl} and u_{pipe} are set to equal, Equation (8) can be rearranged to Equation (9) as shown below¹¹:

$$d_{cyl} = \left[8.442 d_{pipe}^{0.1786} Sc^{0.0857} \left(\frac{\mu}{\rho} \right)^{0.25} u^{-0.25} \right]^{2.333} \quad (9)$$

Equation (8) can be plotted using typical parameter values ($Sc=1,000$, $\mu=0.01$ poise, $\rho=1 \text{ g/cm}^3$, $d=1.2$ cm) as shown in Figure 1. At 5,000 rpm with a rotating coupon having an outer diameter of 1.2 cm, the maximum (tangential) linear velocity on the coupon surface is 3.1 m/s. Figure 2, plotted from Equation (9), shows the relation between the rotating cylindrical coupon diameter in a glass cell and the average flow velocity in a straight pipe.

EXPERIMENTAL PROCEDURE

Desulfovibrio desulfuricans subsp. *desulfuricans* ATCC[®] 7757 was used in this work. Modified ATCC 1249 medium was used for cell growth⁷. The inoculum level of SRB was around 3×10^5 cell/ml. The culture medium preparation, coupon polish and the glass cell experimental procedure were reported previously⁷. To minimize oxygen contamination, a small amount nitrogen was continuously fed to the glass cell during experiments to provide a positive overhead pressure. Cysteine was added as an oxygen scavenger at $0.5 \text{ g}\cdot\text{l}^{-1}$ at the beginning of each run. After about five days, the C1018 coupon was taken out from the glass cell and prepared for surface analysis under a scanning electron microscopy (SEM).

A 2.5% (wt) glutaraldehyde solution was used to immobilize the biofilm on the coupon surface. After 8 hours of immersion in the glutaraldehyde solution, the coupon was successively dehydrated by ethanol with a graded series (30%, 50%, 70%, 100% v/v) followed by critical point drying and gold coating for SEM observation. For the cross-section analysis under SEM, the coupon was mounted in epoxy. After the epoxy was cured, the sample was cut off, and the cross-section of the sample was polished serially using sand paper with 200, 400, 600 and 1500 grits, respectively. Finally, it was polished on a rotating velveteen wheel wetted with $9 \mu\text{m}$ and $3 \mu\text{m}$ diamond suspensions successively. The coupon was then stored in a nitrogen-filled desiccator for SEM observation at a later time.

RESULTS AND DISCUSSION

Our previous work⁷ showed that a mild agitation rate facilitated planktonic cell growth compared to growth in a static liquid medium, probably due to increased mass transfer rates. The mild agitation rate also increased MIC corrosion, while a high agitation rate decreased MIC corrosion compared to the mild agitation rate. The biofilm image analyses in this work corroborated these observations. Kidney-shaped sessile SRB cells were clearly visible on the coupon surfaces for the 0 rpm and 1,000 rpm tests. The sessile SRB cells were embedded in a matrix as shown in Figures 3 and 4. Some methods can be applied to quantify the sessile cells in the biofilms. For example, the sessile cells can be scraped off and

quantified using the Most Probable Number (MPN) method¹⁸ and the quantitative PCR method¹⁹. These methods will be adopted in our future work. For Figure 5, the coupon surface for the rotational speed of 3,000 rpm was quite smooth. No sessile SRB were detected on the prepared coupon surface as seen in Figure 5. The corresponding linear velocity for 3,000 rpm in a 10-inch pipe is estimated to be 3.5 m/s based on Figure 1. The same velocity was used to remove a *P. aeruginosa* biofilm by Stoodley et al.⁵ Figure 5 also shows cracks in a mineral film. An EDS or XRD study is needed to confirm the identity of the film. The images here clearly indicate that there is a relationship between fluid flow and sessile SRB growth on the coupon surface.

Figure 6 shows a cross-section comparison of coupon surfaces at different flow rates. The surface coverage at 3,000 rpm was much thinner than at 1,000 rpm because of the lack of a biofilm at 3,000 rpm as shown on Figure 5. Figure 6 also shows that the base metal surface at 1,000 rpm was more rugged and thus likely more corroded.

Glass cells can provide high flow rates and shear stresses. However at high rotational speeds, centrifugal force becomes significant and it may repel bacteria away from the coupon surface. This deviates from pipe flow conditions for biofilm formation. To validate the experimental results from glass cells, a small-scale flow loop attached to a glass cell (Figure 7) is proposed. The flow channel (a tube) is fitted with multiple coupons. This kind of device is similar to a Modified Robbins Device (MRD) that is commonly used in growing biofilms for environmental engineering and medical research^{20, 21}. The setup can be operated in strictly batch mode without feed and discharge during a run. It can also be run in a continuous mode. To keep supplying fresh nutrients to the biofilms on the coupons, a feed stream is pumped into the bioreactor and a discharge stream is used. Because high linear velocities are used in some of the tests, it is too costly to pump in and out large amounts of liquid. Instead, a recycle loop can be used to provide large flow velocities above the coupon surfaces while keeping the feed and discharge flow rates manageable. The flow rates are regulated with restriction valves. The schematic of a custom-made pipe fitted with five coupons is shown in Figure 8. Each coupon has a contoured surface to allow flush mounting on the pipe wall. The coupons can be independently removed by pulling out the support rod to which the disk coupon is glued. During a coupon's removal, liquid flow is temporarily stopped. The fluid in the pipe is transferred to the glass cell. Filtered nitrogen is then used to provide a positive pressure to prevent air contamination. A large solid rod is inserted into the center of the main pipe to provide annual flow with a much larger average linear velocity above the coupon surfaces. Each coupon will have a diameter of 1.15 cm. This flow loop device will be used in our future work.

CONCLUSIONS

A glass bioreactor with a rotating cylinder coupon was used to study flow effects on SRB biofilm formation. Theoretical derivations showed that the coupon rotational speed could be correlated with the pipe flow velocity using wall shear stress and/or mass transfer similarity. Experimental results in the glass cell inoculated with *D. desulfuricans* indicated that at 3,000 rpm (roughly equivalent to 3.5 m/s in pipe flow) sessile SRB cells could not adhere on the coupon surface to form an SRB biofilm. This provides a guideline for the potential use of shear to prevent biofilm formation. Additional experiments are desired to find a flow velocity that is needed to dislodge an established biofilm.

REFERENCES

1. H. A. Videla, L. K. Herrera, and R. G. Edyvean, An updated overview of SRB induced corrosion and protection of carbon steel, Paper No. 05488, *Corrosion/2005*, NACE International, Houston, TX , 2005.
2. P. F. Sanders, Overview of souring, corrosion and plugging due to reservoir organisms, *UK Corrosion 98*, Paper 15, Sheffield, UK, Oct. 20-21, 1998.
3. W. Lee, and W. G. Characklis, Corrosion of mild steel under anaerobic biofilm, *Corrosion*, 49, 186-198, 1993.
4. P. Stoodley, I. Dodds, J. D. Boyle and H. M. Lappin-Scott, Influence of hydrodynamics and nutrients on biofilm structure, *Journal of Applied Microbiology Symposium Supplement*, 85, 19-28, 1999.
5. P. Stoodley, R. Cargo, C. J. Rupp, S. Wilson and I. Klapper, Biofilm material properties as related to shear-induced deformation and detachment phenomena, *Journal of Industrial Microbiology and Biotechnology*, 29(6), 361-368, 2002.
6. B. C. Dunsmore, A. Jacobsen, L. Hall-Stoodley, C. J. Bass, H. M. Lappin-Scott and P. Stoodley, The influence of fluid shear on the structure and material properties of sulfate-reducing bacteria biofilms, *Journal of Industrial Microbiology and Biotechnology*, 29, 347-353, 2002.
7. J. Wen, K. Zhao, T. Gu and S. Netic, Effects of mass transfer and flow conditions on SRB corrosion of mild steel, Paper No. 06666, *Corrosion/2006*, NACE International, Houston, TX, 2006.
8. D. C. Silverman, Rotating cylinder electrode for velocity sensitivity testing, *Corrosion*, 40, 220-226, 1984.
9. D. C. Silverman, Rotating cylinder electrode –geometry relationships for prediction of velocity-sensitive corrosion, *Corrosion*, 44, 42-49, 1988.
10. D. C. Silverman, The rotating cylinder electrode for examining velocity-sensitive corrosion-a review, *Corrosion*, 60, 1003-1023, 2004.
11. D. C. Silverman, Conditions for similarity of mass-transfer coefficients and fluid shear stresses between the rotating cylinder electrode and pipe, *Corrosion*, 61, 515-518, 2005.
12. K. D. Efird, E. J. Wright, J. A. Boros and T. G. Hailey, Correlation of steel corrosion in pipe flow with jet impingement and rotating cylinder tests, *Corrosion*, 49, 992-1003, 1993.
13. I. H. Shames, *Mechanics of Fluids*, 4th ed., McGraw Hill, New York, 410-414, 2003.
14. R. L. Daugherty, J. B. Franzini and E. J. Finnemore, *Fluid Mechanics with Engineering Applications*, 8th ed., McGraw Hill, New York, 207-209, 1985.
15. R.W. Fox and A.T. McDonald, *Introduction to Fluid Mechanics*, 4th ed., Wiley , p. 350, 1992.

16. G. H. Sedahmed, K. Abdell and A. M. Abdallah, Mass transfer at rotating finned cylinders, *Journal of Applied Electrochemistry*, 9, 563-566, 1979.
17. D. A. Shaw and T. J. Hanratty, Turbulent mass transfer rates to a wall for large Schmidt numbers, *AIChE Journal*, 23, 28-37, 1977.
18. H. A. Videla, *Manual of Biocorrosion*, Lewis Publishers, Boca Raton, 1996.
19. X. Zhu, J. II. Kilbane, A. Ayala and H. Modi, Application of quantitative, real-time PCR in monitoring microbiologically influenced corrosion (MIC) in gas pipelines, Paper No. 05493, *Corrosion/2005*, NACE International, Houston, TX, 2005.
20. C. J. Linton, A. Sherriff1 and M. R Millar, Use of a modified Robbins device to directly compare the adhesion of *Staphylococcus epidermidis* RP62A to surfaces, *Journal of Applied Microbiology*, 86, 194–202, 1999.
21. W. F. McCoy, J. D. Bryers, J. D. Robbins and J. W. Costerton, Observations of fouling biofilm formation, *Canadian Journal of Microbiology*, 27, 910–917, 1981.

**TABLE 1
TEST MATRIX**

Microorganism	<i>Desulfovibrio desulfuricans</i> (ATCC 7757)
Test medium	Modified ATCC 1249 medium
Oxygen scavenger (cysteine) (g/L)	0.5
Coupon material	UNS C1018
Temperature (°C)	37
pH	7.0±0.1
Rotational speed (rpm)	0, 1,000, 3,000

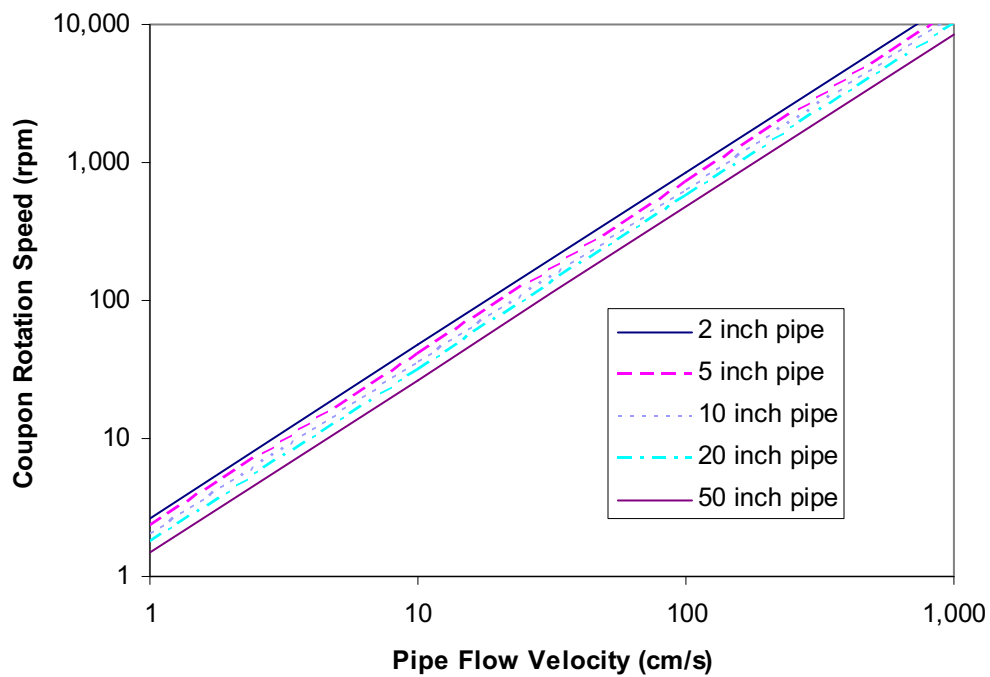


FIGURE 1 - Relation between rotational speed in glass cell and average flow velocity in a straight pipe based on Equation (8).

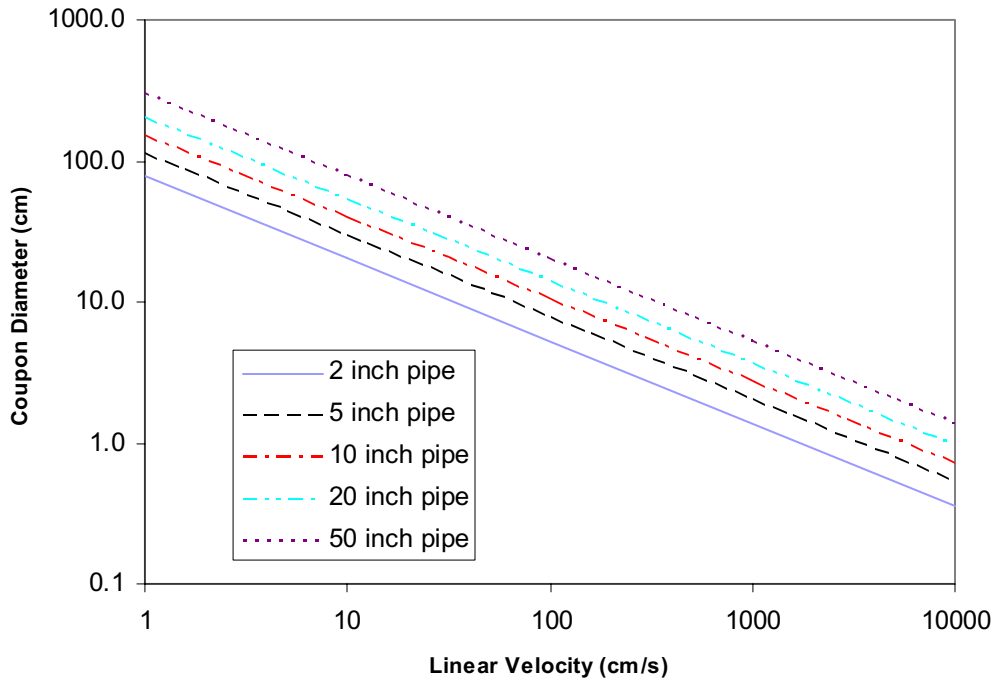


FIGURE 2 - Relation between rotating cylindrical coupon diameter in glass cell and average flow velocity in a straight pipe based on Equation (9).

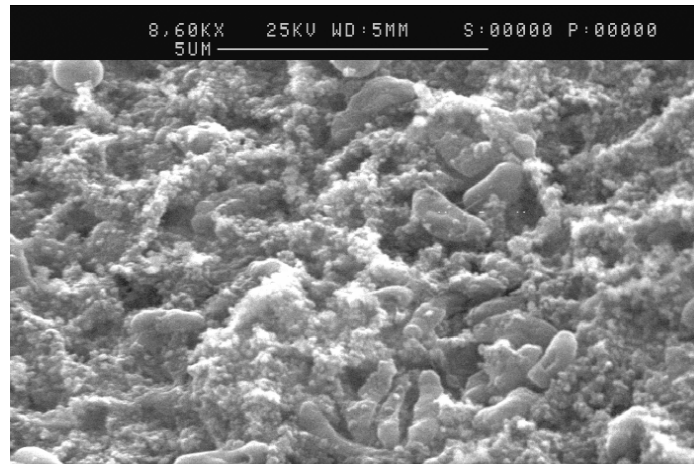


FIGURE 3 - SEM biofilm image on coupon surface for 0 rpm rotational speed at 8,600X magnification.

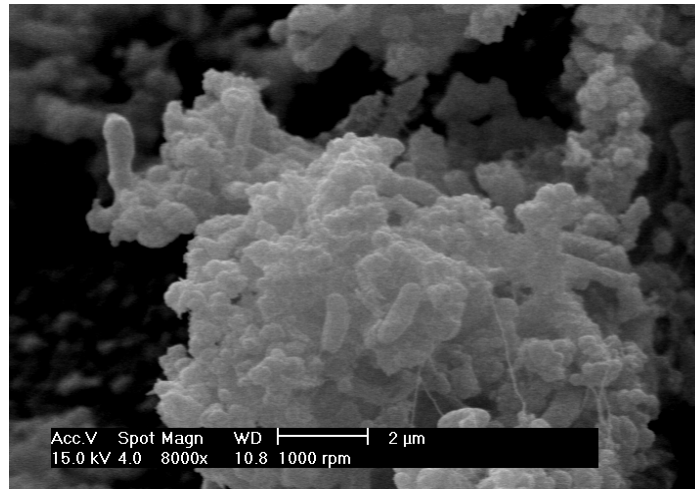


FIGURE 4 - SEM biofilm image on coupon surface for 1,000 rpm rotational speed at 8,000X magnification.

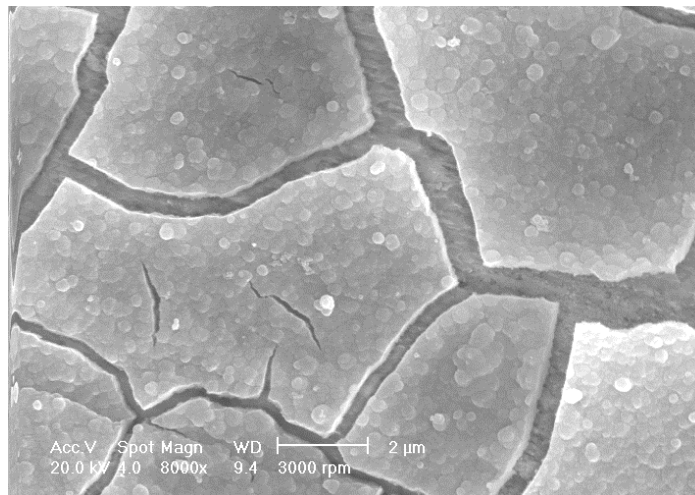
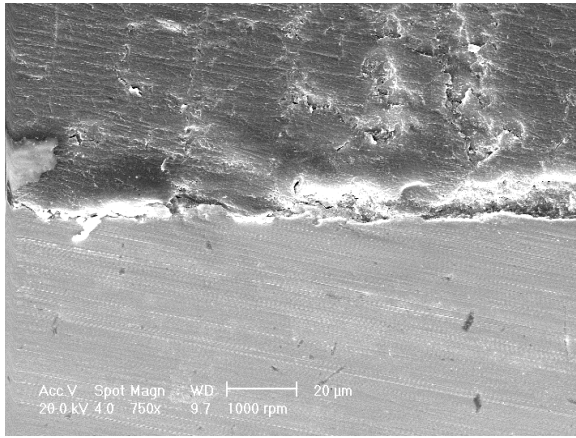
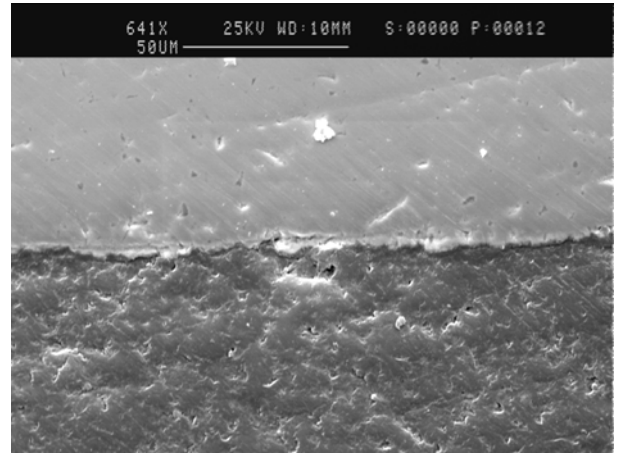


FIGURE 5 - SEM biofilm image on coupon surface for 3,000 rpm rotational speed at 8,000X magnification.



(a) 1,000 rpm, 750X



(b) 3,000 rpm, 641X

FIGURE 6 - Comparison of coupon cross-sections at different rotational speeds: a) 1,000 rpm; b) 3,000 rpm.

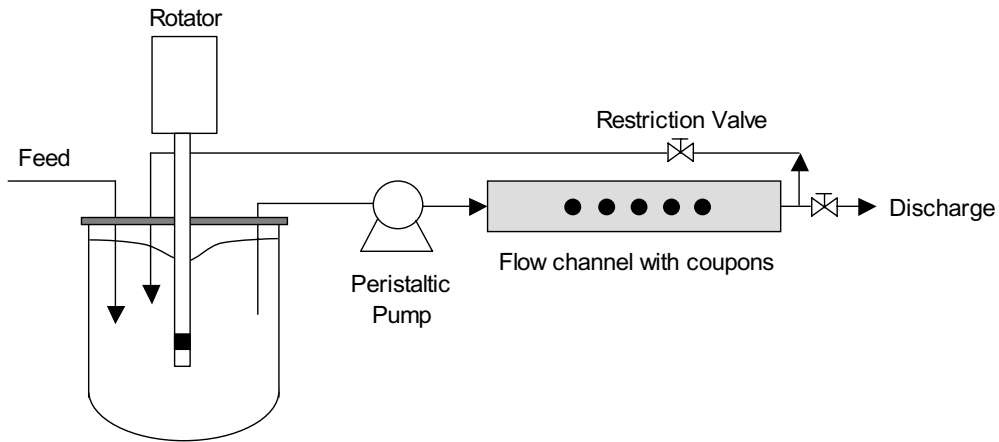


FIGURE 7 - A flow loop attached to an electrochemical glass cell bioreactor.

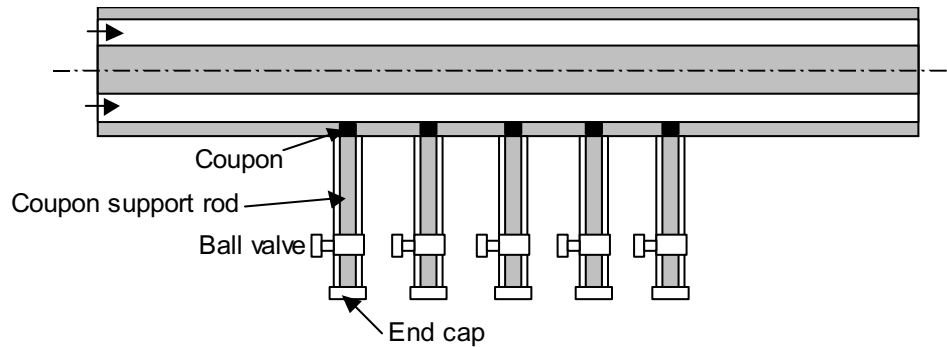


FIGURE 8 - Schematic diagram of an annular flow channel with five flush mounted coupons.